Measurement and Evaluation of Partial Discharge Inception Voltage for Enameled Rectangular Wires under AC Voltage

Toru Wakimoto[1,2], Hiroki Kojima[1] and Naoki Hayakawa[1]

[1] Department of Electrical Engineering and Computer Science
Nagoya University, Furo-cho, Chikusa-ku, Nagoya 464-8603, Japan
[2] NIPPON SOKEN, Inc., 14, Iwaya, Shimohasumi-cho, Nishio 445-0012, Japan

ABSTRACT

Recently, the market for EVs (Electric vehicles) and HEVs (Hybrid electric vehicles) has been expanding. In these vehicles, rectangular wires have started to be used for the traction motor coil to increase the motor performance. As a result, the insulation techniques become important because the applied voltage between the wires is increasing due to a change in the motor structure and the increase in the driving voltage. In order to safeguard the motor insulation, partial discharge (PD) between coil wires must be controlled, and to do this, the coil wires should be coated with an insulator of a suitable thickness. For this purpose, the PD measurement technique is important in design and inspection on the manufacturing lines. However, the PD measurement between wires is unstable, and is especially affected by the measurement method and environmental factors. In this paper, we clarify the factors as well as the mechanism affecting the PD inception voltage (PDIV) between enameled rectangular wires under AC voltage. The effects of the ambient humidity, the pre-discharge conditions and the measuring frequency on the PDIV were analyzed. As a result, it was confirmed that when there was pre-discharge in a high humidity environment, the PDIV displayed fluctuating characteristics in which it momentarily decreased and then increased. We observed the discharges and analyzed the electric field distribution. The results showed that in high humidity environment, pre-discharge causes moisture contained in the air to adhere to the coating surfaces, resulting in an increase in the surface conductivity, which influences the electric field strength in the air gap between coil wires. These analyses indicated that the PDIV can be measured stably and reliably at high frequencies in a high humidity environment.

Index Terms - **Partial discharges, environmental factors, enamel insulated wires, motors, insulation testing.**

1 INTRODUCTION

RECENTLY because of the increased demand for higher performance in motors for EVs and HEVs, rectangular wires have started to be used in motor coils to increase the space factor in the motor stator. Subsequently, because of the requirements associated with a high-voltage drive, the insulation coatings on the coil wires have been made thicker. With this type of wire material, understanding the partial discharge (PD) characteristics and achieving a more controlled insulation design are quite important for EVs and HEVs to achieve a sufficient level of performance.

Methods of measuring the PD between the coil wires have been discussed, including electrical methods [1, 2], electromagnetic methods [3, 4], and others. Existing research related to the PD characteristics in motors includes some examples in which the ambient humidity was changed [5, 6]. It has been pointed out in the research that the PDIV decreases in high-humidity environments, and as a result, the decrease in the withstand voltage of the air and the decrease in the surface resistance can lead to a decrease in the charge accumulated on the wire surface.

In designing motor insulation and motor manufacturing lines, the PDIV between coil wires is measured under an AC voltage to evaluate the insulation performance of the motor coil wires. Therefore, it is important to measure the PDIV stably and reliably. For this purpose, it is useful to clarify the effects on the PDIV of factors including the measurement environment (especially ambient humidity) and the measurement method, which involves the measurement frequency and the pre-discharge time for repeated measurements. This paper focuses on the ambient humidity, pre-discharge and measuring frequency in order to

Manuscript received on 18 September 2015, in final form 9 August 2016, accepted 10 August 2016.

clarify both the mechanism and the effect of these factors on the PDIV characteristics between rectangular wires.

2 EXPERIMENTAL SETUP

2.1 PD DETECTION CIRCUIT AND TEST SAMPLE

The setup for PD measurement is shown in Figure 1. The PDIV was measured under an AC voltage by preparing the test sample shown in Figure 2, where one wire was bent and a plastic clip was used to establish contact between the wires. The clipping force was 7.8 N which is low enough to avoid deformation of coatings. The applied voltage and frequency were changed using a high-speed, high-voltage amplifier and a function generator. The PDs in the test sample go through a 200-pF coupling capacitor to a CR circuit. The amplitude of the output voltage of the CR circuit was measured as the PD signal. The PD signal was initially calibrated using a pulse generator with various charge amounts. The reason why there are two CR circuits in the measurement circuit is to differentiate the PD signal from the noise components for the polarity of the detected waveform.

The wires evaluated in this experiment were made of rectangular wire with a polyimide amide (AIW) coating that was 40 μm or 160 μm thick. The shapes of the two sample wires were 2.3 mm × 1.5 mm (40 μm thick) and 2.8 mm × 2.1 mm (160 μm thick) as shown in Table 1. These coating thickness were decided from the range of variation in the actual motor used in the commercial product. Inside of the both coatings, voids or impurity matters were scarcely contained with regard to the specifications of wires, and the roughness of the both coatings were less than 1 μm according to the photograph of cross section of coatings. The test sample was cleaned with alcohol and placed in a thermo-hygrostat as the prior treatment. In order to analyze the PD location during PDIV measurement, PD luminescence image was observed through a window using a high-sensitivity camera.

2.2 EXPERIMENTAL PROCEDURE

The conditions and procedure for PD measurement are shown in Table 2 and Figure 3. A pre-discharge voltage of 1 kHz at a fixed voltage equal to 1.2 × initial PDIV at 1 kHz was applied for 5–60 s, and the pre-discharge was stopped momentarily for PDIV measurements at 5 Hz, 50 Hz and 1 kHz, respectively. By repeating the above procedure, the change in the PDIV as a function of the total pre-discharge time and the PDIV characteristics as a function of the measuring frequency were evaluated. The voltage was increased by 20 V/s for the PDIV measurement, and the PDIV was judged to be the peak voltage in the cycle at which one PD pulse higher than 5 pC occured. The PDIV measurement was performed five times at the same condition, and the average value, maximum value, and minimum value were evaluated. After the PDIV evaluations, the PD locations were also observed for sample A when the applied voltage was set to the PDIV. The PD luminescence image was captured at an exposure time of 0.45 s.

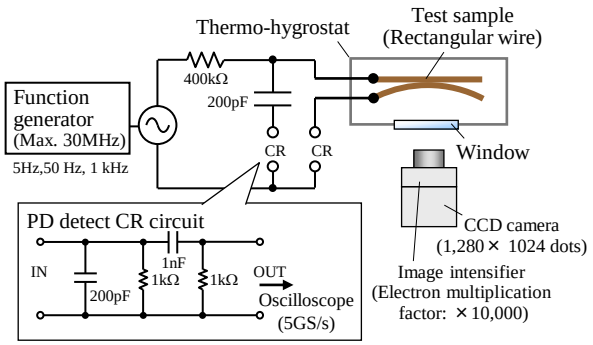

Figure 1. Experimental setup.

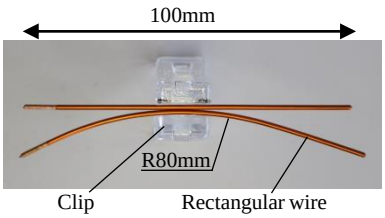

Figure 2. Test sample.

Table 1. Specifications of rectangular wires.

	Sample A	Sample B
Size	2.3 × 1.5 mm	2.8 × 2.1 mm
Coating thickness	40 μm	160 μm
Coating material	AIW	AIW
Permittivity of coating	4.0	4.0

Table 2. Conditions for PD measurement

Environmental conditions	25 °C / 20 %RH, 90 %RH
Pre-discharge conditions	1 kHz, 1.2 × PDIV @ 1 κHz
PDIV measurement frequency	5 Hz, 50 Hz, 1 kHz
PD detection sensitivity	5 pC
Voltage rise/ decrease speed	20 V/s

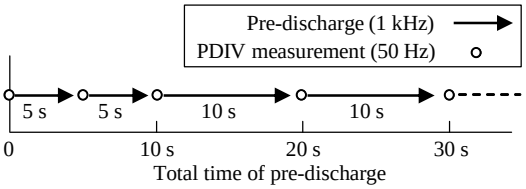

Figure 3. PDIV measurement procedure.

3 EXPERIMENTAL RESULTS

3.1 PDIV CHANGE UNDER PRE-DISCHARGE

Figure 4 shows the measurement results for the PDIV as a

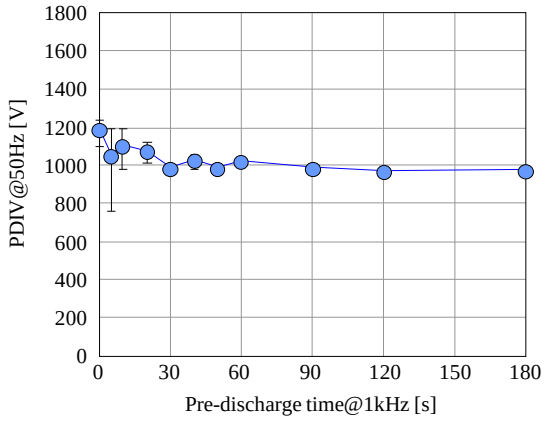

(a) Sample A

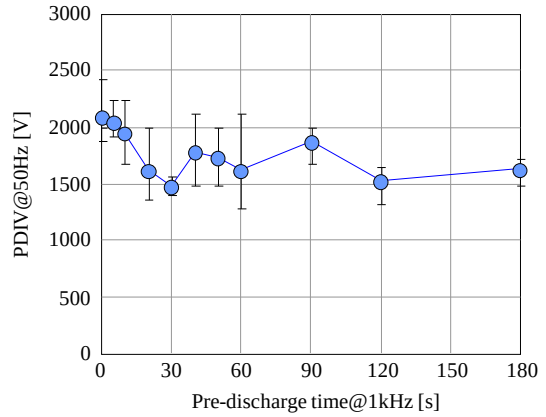

(b) Sample B

Figure 4. PDIV as a function of pre-discharge time (20 %RH).

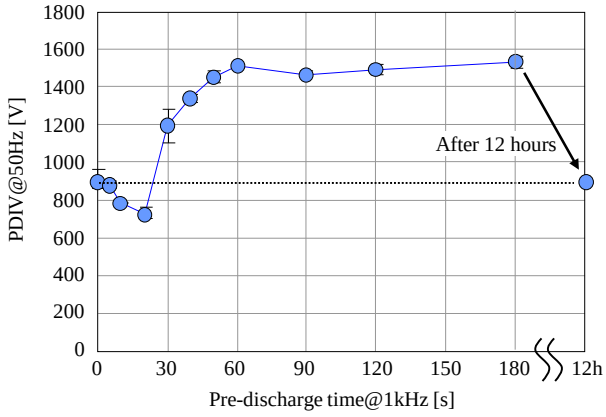

(a) Sample A

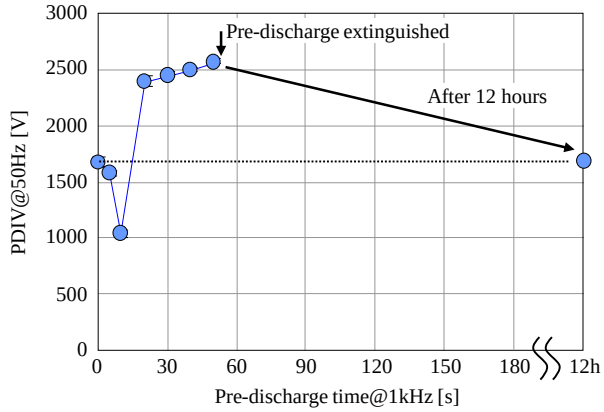

(b) Sample B

Figure 5. PDIV as a function of pre-discharge time (90 %RH).

function of the total pre-discharge time for samples A and B under a 20 %RH environment. In each case, the PDIV as a function of the pre-discharge time was relatively stable, though it shows a slight scattering between the maximum and minimum values during the initial period of pre-discharge.

Similarly, Figure 5 shows the measurement results under 90 %RH. For the sample A, the PDIV (at 50 Hz) decreased in the initial period up to the pre-discharge time of 20 s, but the PDIV increased significantly for pre-discharge times of 30 s or more, and then saturated. The results show the same trend for the sample B. For the sample B, the PDIV decreased in the initial period up to a pre-discharge time of 10 s and increased after a pre-discharge time of 20 s. When the pre-discharge time exceeded 50 s, the pre-discharge was extinguished, and the test was concluded.

At both samples, the second test at 90 %RH was performed 12 hours after the first test. As a result, the PDIV was confirmed to reproduce the initial values in Figures 4 and 5.

3.2 FREQUENCY CHARACTERISTICS OF PDIV

Figure 6 shows the frequency dependence of the PDIV at 90 %RH for both samples at pre-discharge times of 0 s, 10 s and 30 s. At a pre-discharge time of 0 s in Figure 6a, the PDIV is stable with a small scattering with frequency. However, at a pre-discharge time of 10 s in Figure 6b, the PDIV decreased as the frequency decreased. On the other hand, at a pre-discharge time of 30 s in Figure 6c, the PDIV increased as the frequency decreased for both samples.

The above results confirm that the PDIV and its frequency characteristics vary with the pre-discharge time in a high-humidity environment of around 90 %RH.

3.3 CHANGE OF PD LOCATIONS

Figure 7 shows the PD luminescence images during the PDIV measurement at 50 Hz in an environmental humidity of 20 %RH and 90 %RH. As shown in this figure, at 20 %RH, the PDs were close to the contact point of the wires, and no changes were seen with elapsed time. In contrast, at 90 %RH, the PDs changed with the pre-discharge time. At a pre-discharge time of 10 s when the PDIV decreased, PDs were observed closer to the contact point (shorter gap side). However, after 30 s when the PDIV rose, the PD locations changed and spread outward (longer gap side) from the contact point.

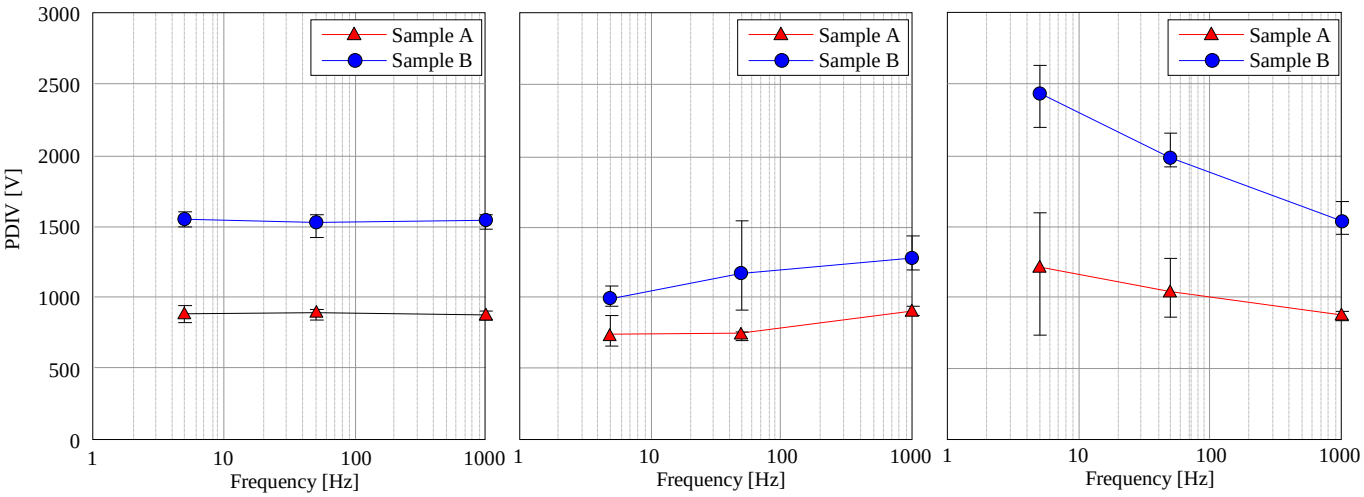

(a) Pre-discharge time 0s (b) Pre-discharge time 10s (c) Pre-discharge time 30s

Figure 6. Frequency dependence of PDIV for different insulation thickness and pre-discharge time (90 %RH).

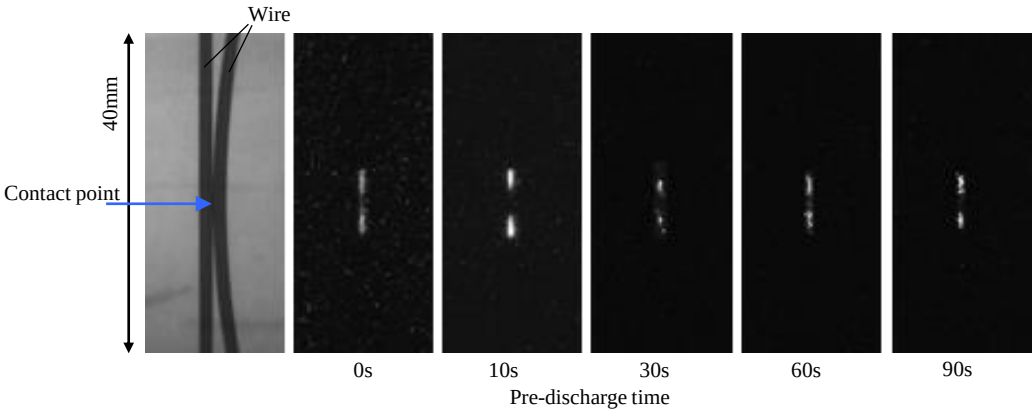

(a) 20 %RH

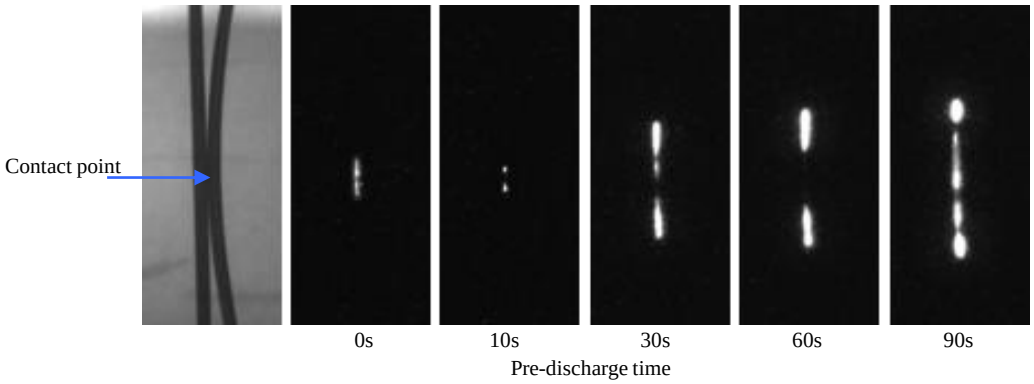

(b) 90 %RH

Figure 7. PD luminescence images for different ambient humidity (at PDIV @ 50 Hz, Sample A)

4 MECHANISM ANALYSIS

4.1 FACTORS IN PDIV CHANGES

Possible factors in the changes in the PD characteristics in the previous section are, for example, corrosion of the coating [7, 8] and charge accumulating on the coating surface [9, 10], and especially in paper [9], “conditioning” which conducted pre-discharge before measurement is suggested to generate stable condition of surface charge. According to these reports, the measurement results at 20 %RH in Figure 4 can be concerned by surface charge. However, the measurement results at 90 %RH in Figure 5 cannot be explained by previous

knowledge. Therefore in this research, the authors focused on the phenomenon of the change in the PDIV at high humidity, and analysis was carried out to clarify the mechanism.

The coating thickness measured after the PDIV measurement in Figure 5a decreased by a maximum of only 0.7 μm against an initial coating thickness of 40 μm. Moreover, as shown by the measurement result in Figure 5, even if the PDIV changed in a high-humidity environment due to pre-discharge, it returned to its initial value within 12 hours after the end of measurements. For these reasons, PDIV changes in a high-humidity environment can be related to a chemical modification of the surface coatings, in particular, the surface conductivity.

Many arguments have been put forward to explain surface chemical modification in the plastic materials field. Particularly, researches concerning modification of the surface characteristics of polymeric film, which changes from hydrophobic to hydrophilic, have been reported [11-13]. From these reports, the surface of the polymeric film is modified by a corona discharge and made hydrophilic, i.e. the plasma produced by the electric discharge collides with the film surface and cuts the polymer chain, which combines with atmospheric oxygen. As a result, a hydroxyl group or a carboxyl group with hydrophilic characteristics is formed on the polymeric film. On the other hand, polymers such as polyimide used for the wire coatings in this measurement are known as highly absorptive substances [14, 15]. Moreover, the state of the modified surface will not be maintained for a long time, especially in the state where the surface modification decreases quickly in the initial period after the modification stops [16]. For these reasons, in this experiment, it is considered that the pre-discharge modified the coating surface and made it hydrophilic, and thus moisture contained in the air adhered to its surface. Consequently, the conductivity of the coating surface increased and affected the electric field in the air gap as shown in Figure 8. To confirm this assumption, the electric field is analyzed in the next sub-section.

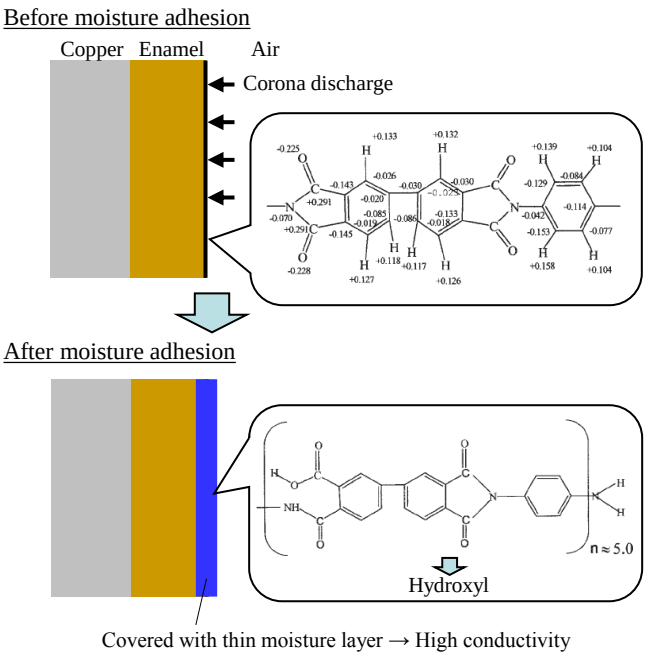

Figure 8. Mechanism of moisture in the air to adhere to coating surface[12].

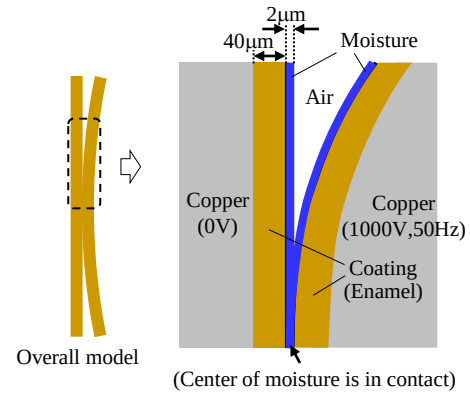

Figure 9. Calculation model for electric field distribution.

4.2 CALCULATION MODEL FOR ELECTRIC FIELD DISTRIBUTION

The electric field strength in the air gap between the wires was calculated by finite element method under an AC voltage. Figure 9 shows the two-dimensional basic structure of the calculation model with a wire coating thickness of 40 μm, in which the coating surfaces are assumed to be covered by a moisture layer with a thickness of 2 μm in different patterns. Table 3 shows the physical constants of the calculation model. With this model, the electric field strength in the air gap was calculated when 1,000 V was applied between the conductors at different frequencies (5 Hz, 50 Hz and 1 kHz).

The electrical conductivity of moisture σ_w (= 1.0×10^{-3} S/m) was set from the following preliminary calculation with the model where the entire coating surface is covered with a moisture layer. Figure 10 shows the electric field strength in the middle of the air gap at a gap length of 40 μm as a function

Table 3. Physical constants of calculation model.

	Relative Permittivity ε_r	Conductivity σ_W [S/m]
Copper	-	5.9×10^{7}
Enamel	4.0	0
Air	1.0	0
Moisture	80.0	1.0×10^{-3}

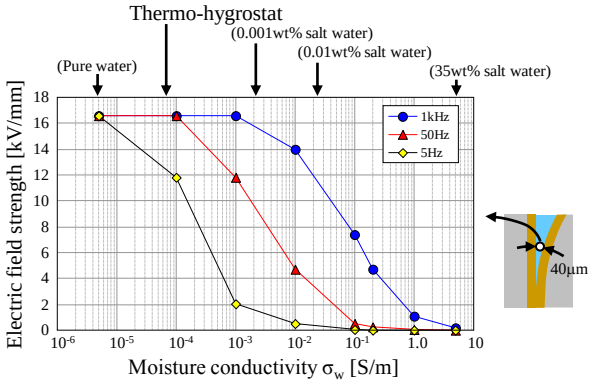

Figure 10. Electric field strength in air gap as a function of moisture conductivity.

of σ_w for different frequencies. This air gap length of 40 μm refers to the location where the PDs began to occur based on Paschen's law, which is derived from the point of contact between the electric field strength in the air gap and the Paschen curve [17]. The electric field strength decreases as the frequency decreases or as σ_w increases. In this analysis, we used $\sigma_w = 1.0 \times 10^{-3}$ S/m near to 0.001wt% salt water for the electrical conductivity of moisture layer on the coating surfaces.

4.3 ELECTRIC FIELD DISTRIBUTION AT HIGH HUMIDITY

4.3.1 IN CASE OF MOISTURE LAYER ATTACHED TO COIL COATING EXCEPT CONTACT POINT

As described above, PDs can occur at the location of the 40 μm air gap in the initial period of pre-discharge. As a result, the electric field and the PDIV can change at high humidity, when moisture contained in the air exists near the coating surfaces where the PDs occurred initially. The authors calculated the electric field strength with moisture layers attached to the coil coatings. Figure 11 shows the electric field distribution for different frequencies calculated from the model that includes the moisture layer partially with a length of 1.5 mm. This moisture length is set to contain the PD inception point at the gap length of 40 μm shown in Figure 11. The electric field strength along its center line in the air gap is plotted in Figure 12. In this figure, the electric field strength at the area where moisture exists increases when the location becomes closer to the contact point, compared with the model that does not include moisture, and these changes were found to be significant at lower frequencies.

When the moisture changes the electric field distribution in Figure 12, the areas in which PDs occur may also change, because the relationship between the electric field strength in the air gap and the Paschen curve will change as shown in Figure 13. The electric field distribution in the air gap was plotted for the model with and without moisture, respectively, at 50 Hz. The applied voltage for both curves was set to the PDIV in each case, i.e. the value to make contact with the Paschen curve. According to this result, the PDIV in the model with moisture (680 V) is lower than the model without moisture (840 V), and the point at which PDs occur shifts toward the shorter gap length and the contact point. This result is consistent with the fact that the PDIV decreased and PDs were observed closer to the contact point during the first stage of pre-discharge in Figures 5a and 7b. After repeating this process, the PD location will shift toward the contact point, and then the moisture layer on the coating surfaces will extend to the contact point. At this moment, the electric field distribution in the air gap and PDIV characteristics may change significantly, so that in the next sub-section, the electric field distribution is calculated when the moisture layer reaches the contact point.

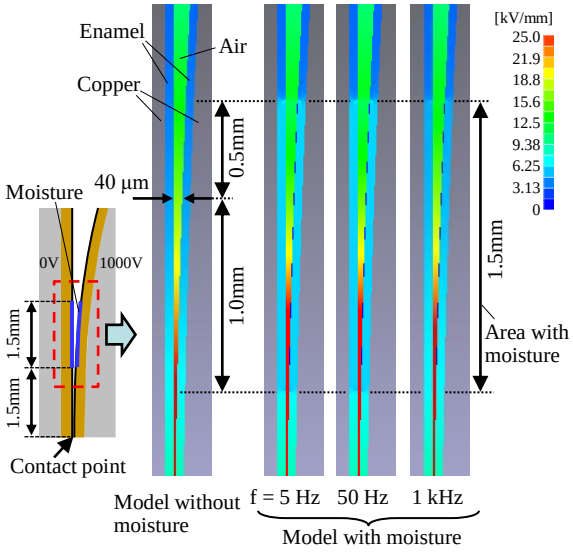

Figure 11. Electric field distribution for different frequencies (Moisture layer is attached to coil coating except contact point).

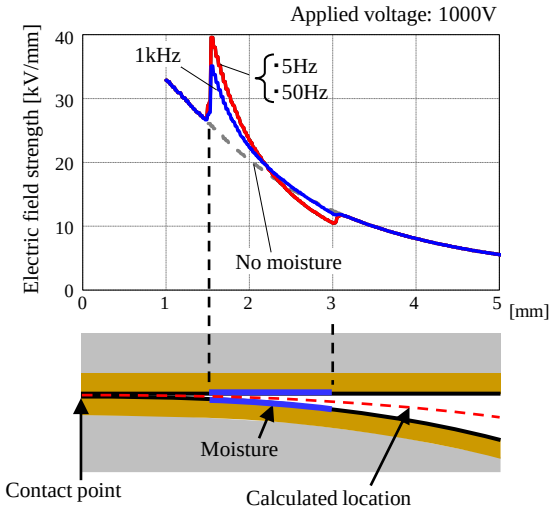

Figure 12. Electric field strength when moisture layer is attached to coil coating except contact point.

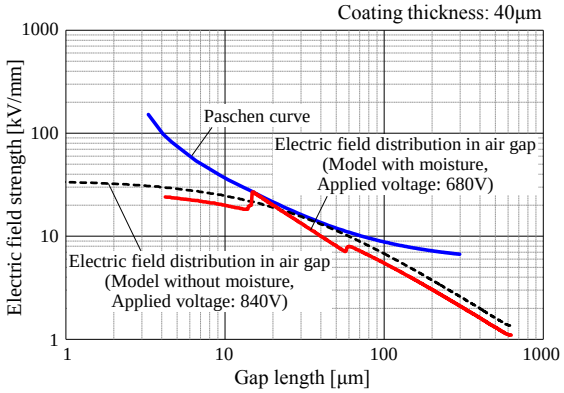

Figure 13. Relationship between electric field distribution in air gap and Paschen curve (Moisture layer is attached to coil coating except contact point).

4.3.2 IN CASE OF MOISTURE LAYER ATTACHED TO COIL COATING CONTAINING CONTACT POINT

Figure 14 shows the calculation results for the electric field distributions when the moisture layer on the coating surfaces reached the contact point, i.e. the moisture length is 3.0 mm from the contact point. In addition, the electric field strength in the air gap using the same procedure as in the previous figures is shown in Figures 15 and 16. In contrast to Figures 11 and 12, the electric field strength in the air gap is reduced by the moisture layer, and its value decreases with decreasing frequency as shown in Figures 14 and 15. As a result, the PDIV in the model with moisture (950 V) is higher than the model without moisture (840 V), and the PD location shifts toward the longer gap length as shown in Figure 16.

4.4 MECHANISM OF PDIV CHANGES WITH PRE-DISCHARGE AT HIGH HUMIDITY

The results of analyses on electric field distribution clarify the following three important points: Firstly, the electric field strength in the air gap actually changes when moisture exists on the wire coating surfaces, and the electric field distribution changes depending on the area in which moisture exists. This can be the main reason why the PDIV changes with the pre-discharge in Figure 5. Secondly, the above phenomenon becomes more significant at low frequencies, i.e. when the surface conductivity affects complex dielectric constant ($\sigma+j\omega\varepsilon$). This can be the reason why the change in the PDIV decreases or increases at lower frequencies in high humidity environment in Figures 6b or 6c. And thirdly, the PD location at the PDIV measurement at 50 Hz changes depending on the area in which moisture exists. When moisture exists on a part of the wire coating surface, PDs occur near the contact point of the wires due to the local enhancement of the electrical field strength. On the other hand, when moisture reaches the contact point, PDs occur away from the contact point due to the decrease in the electric field strength in the area in which moisture exists. This can be the reason for the change in the PD location with the pre-discharge in Figure 7b.

Based on the above experiments and analyses, the PDIV change in the high humidity environment measured in Figure 5 can be schematically explained in Figure 17. In the initial pre-discharge period, PDs occurred in the air gap between the coil wires, and they partially activated the coating surfaces. As a result, the coating surfaces became hydrophilic, allowing the moisture contained in the air to partially condense on the coating surfaces. This leads to the local enhancement in the electric field strength around the moisture layer on the coating surfaces, which decreased the PDIV and shifted the PD location toward the contact point in the second period of pre-discharge (~20 s). Subsequently, the moisture reached the contact point, which leads to the decrease in the electric field strength in the air gap, which increased the PDIV and shifted the PD location away from the contact point in the third period of pre-discharge (~20 s).

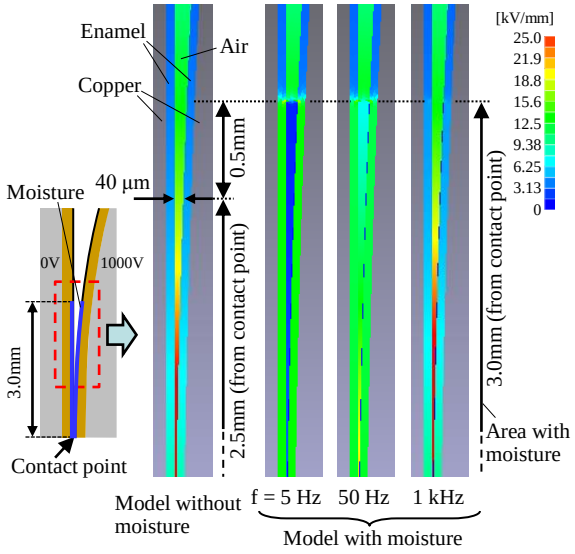

Figure 14. Electric field distribution for different frequencies (Moisture layer is attached to coil coating containing contact point).

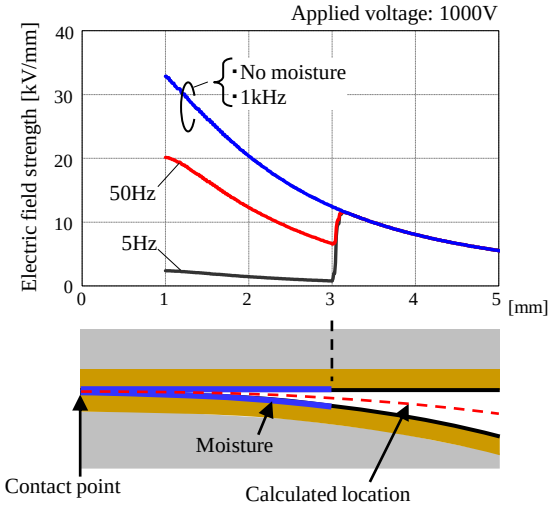

Figure 15. Electric field strength when moisture layer is attached to coil coating containing contact point.

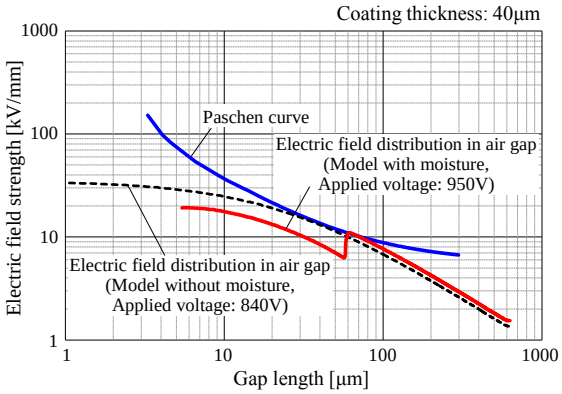

Figure 16. Relationship between electric field distribution in air gap and Paschen curve (Moisture layer is attached to coil coating containing contact point).

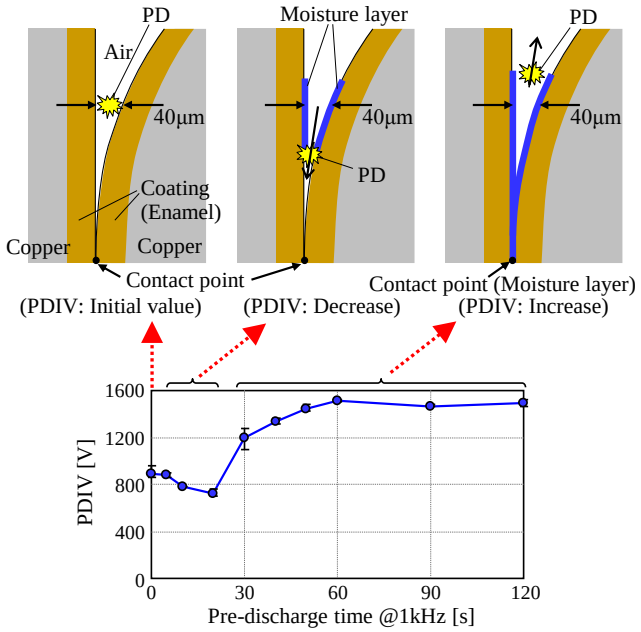

Figure 17. Change of moisture adhesion area, PD location and PDIV value for pre-discharge time at high humidity.

From these findings, the following measurement methods will contribute to the evaluation of PDIV with a small scattering: In a low humidity environment, pre-discharge to generate stable condition of surface charge will be effective as mentioned in section 4.1. On the other hand, in a high humidity environment, a higher frequency which can suppress the change of the electric field distribution in the air gap will be effective as analyzed in Figures 6, 12 and 15.

5 CONCLUSION

This paper investigated the factors as well as the mechanism affecting the PDIV between enameled rectangular wires under AC voltage. The main results are summarized as follows:

(1) The PDIV and its frequency characteristics as well as PD locations vary with the pre-discharge time in a high humidity environment of around 90 %RH.

(2) The pre-discharge caused the moisture adhesion to the wire coating surface and increased the surface conductivity, which influenced the electric field strength in the air gap between coil wires.

(3) The variation in PDIV and PD locations was consistent with the moisture adhesion pattern on the wire coating surface during the pre-discharge.

These findings suggest a useful measuring technique of PDIV between coil wires in consideration of ambient humidity, pre-discharge and measuring frequency. Especially, pre-discharge in a low humidity environment and a higher frequency in a high humidity environment will be effective for the stable and reliable PDIV measurement.

REFERENCES

[1] P. Bidan, T. Lebey, and C. Neacsu, “Development of a new off-line test procedure for low voltage rotating machines fed by adjustable speed drives (ASD)”, IEEE Trans. Dielectr. Electr. Insul., Vol. 10, pp. 168-175, 2003.

[2] F. Guastavino, A. Dardano, and E. Torello, “Measuring partial discharges under pulsed voltage conditions”, IEEE Trans. Dielectr. Electr. Insul., Vol.15, pp.1640 - 1648, 2008.

[3] Y. Shibuya, S. Matsumoto, T. Konno, and K. Umezu, “Electromagnetic waves from partial discharges in windings and their detection by patch antenna”, IEEE Trans. Dielectr. Electr. Insul., Vol. 18, No. 6, pp. 2013-2023, 2011.

[4] D. Fabiani, A. Cavallini, and G. C. Montanari, “A UHF Technique for advanced PD measurements on inverter-fed motors”, IEEE Trans. on Power Electronics, Vol. 23, pp. 2546 - 2556, 2008.

[5] M. Fenger and G.C. Stone, “Investigations into the effect of humidity on stator winding partial discharges”, IEEE Trans. Dielectr. Electr. Insul., Vol.12, pp.341 - 346, 2005.

[6] Y. Kikuchi, T. Murata, Y. Uozumi, N. Fukumoto, M. Nagata, Y. Wakimoto and T. Yoshimitsu, “Effects of Ambient Humidity and Temperature on Partial Discharge Characteristics of Conventional and Nanocomposite Enameled Magnet Wires”, IEEE Trans. Dielectr. Electr. Insul., Vol. 15, No. 6, pp.1617-1625, 2008.

[7] H. Kikuchi and H. Hanawa, “Inverter Surge Resistant Enameled Wire with Nanocomposite Insulating Material”, IEEE Trans. Dielectr. Electr. Insul., Vol. 19, No. 19, pp.99-106, 2012.

[8] N. Hayakawa, H. Inano, Y. Nakamura and H. Okubo, “Time Variation of Partial Discharge Activity Leading to Breakdown of Magnet Wire under Repetitive Surge Voltage Application”, IEEE Trans. Dielectr. Electr. Insul., Vol. 15, No. 6, pp.1701-1706, 2008.

[9] K. Kimura, S. Ushirone, T. Koyanagi and M. Hikita, “PDIV Characteristics of Twisted-Pair of Magnet Wires with Repetitive Impulse Voltage”, IEEE Trans. Dielectr. Electr. Insul., Vol. 14, No. 3, pp.744-750, 2007.

[10] D. Fabiani, G. C. Montanari, A. Cavallini and G. Mazzanti, “Relation between space charge accumulation and partial discharge activity in enameled wires under PWM-like voltage waveforms”, IEEE Trans. Dielectr. Electr. Insul., Vol. 11, No. 3, pp.393-405, 2004.

[11] N. Inagaki, S. Tasaka, K. Narushima and K. Teranishi, “Surface Modification of Poly(tetrafluoroethylene) with Pulsed Hydrogen Plasma”, J. Appl. Polymer Sci., Vol. 83, pp.340-348, 2002.

[12] M. Tahara, N. K. Cuong and Y. Nakashima, “Improvement in Adhesion of Polyethylene by Glow-discharge Plasma”, Surface and Coatings Technology, 173-174, pp.826-830, 2003.

[13] T. Ogawa, S. Baba and Y. Fujii, “Improvement of Bond Strength of BPDA-PDA-Type Polyimide Film by Corona Discharge Treatment”, J. Appl. Polymer Sci., Vol. 100, pp.3403-3408, 2006.

[14] G. Guerrica-Echevarra, J. I. Eguiazabal and J. Nazabal, “Water Sorption in Polyamide 6/Poly(Amino-ether) Blends. II. Mechanical Behavior”, J. Macromolecular Sci., Vol. A40, No.7, pp.705-714, 2003.

[15] V. Miri, O. Persyn, J. M. Lefebvre and R. Seguela, “Effect of water absorption on the plastic deformation behavior of nylon 6”, European Polymer J., Vol. 45, Iss. 3, pp.757-762, 2009.

[16] J. M. Grace and L. J. Gerenser, “Plasma Treatment of Polymers”, J. Dispersion Sci. Technology, Vol. 24, Iss. 34, pp.305-341, 2003.

[17] M. Kaufhold, H. Auinger, M. Berth, J. Speck and M. Eberhardt: “Electrical Stress and Failure Mechanism of the Winding Insulation in PWM-Inverter-fed Low-Voltage Induction Motors”, IEEE Trans. Industrial Electronics, Vol.47, No.2, pp.396-402, 2000.

Toru Wakimoto was born on 4 December 1970. He received the Ph.D. degree in electrical engineering and computer science from Nagoya University in 2016. He joined Denso Corporation in 1993, and temporarily transferred to Nippon Soken Incorporated. He has been engaged in research and development of motors for HEVs. Dr. Wakimoto is a member of the IEE of Japan.

Hiroki Kojima (M'11) was born on 7 December 1975. He received the Ph.D. degree in energy engineering and science from Nagoya University in 2004. Since 2004, he has been at Nagoya University and presently he is an Associate Professor in the Department of Electrical Engineering and Computer Science at Nagoya University. Dr. Kojima is a member of the IEE of Japan.

Naoki Hayakawa (M'90) was born on 9 September in 1962. He received the Ph.D. degree in electrical engineering from Nagoya University in 1991. Since 1990, he has been at Nagoya University and presently he is a Professor in the Department of Electrical Engineering and Computer Science at Nagoya University. From 2001 to 2002, he was a guest scientist at the Forschungszentrum Karlsruche/Germany. Prof. Hayakawa is a member of CIGRE and the IEE of Japan.